Inter J Nav Archit Oc Engng (2011) 3:1~8
DOI 10.3744/JNAOE.2011.3.1.001

Comparison of CFD simulations with experimental data for a tanker model advancing in waves

Hideo Orihara

Technical Research Center, Universal Shipbuilding Co., Mie, Japan

ABSTRACT: *In this paper, CFD simulation results for a tanker model are compared with experimental data over a range of wave conditions to verify a capability to predict the sea-keeping performance of practical hull forms. CFD simulations are conducted using WISDAM-X code which is capable of unsteady RANS calculations in arbitrary wave conditions. Comparisons are made of unsteady surface pressures, added resistance and ship motions in regular waves for cases of fully-loaded and ballast conditions of a large tanker model. It is shown that the simulation results agree fairly well with the experimental data, and that WISDAM-X code can predict sea-keeping performance of practical hull forms.*

KEY WORDS: CFD; WISDAM-X; Added Resistance; Surface Pressures.

INTRODUCTION

In recent years, importance has been recognized increasingly for the reduction of fuel consumption of ships in a seaway to reduce green-house gas emissions from shipping. From a ship design viewpoint, it is of crucial importance to establish reliable prediction methods for ship's propulsive power under realistic wave conditions and to realize their application to the development of hull-forms with superior sea-going capability. In order to achieve these objectives, Universal Shipbuilding Corporations has developed an unsteady CFD ship motion simulation method and has used it as a tool for the development of high-performance hull forms under realistic sea conditions.

One of the advantages of the use of CFD is that they can directly treat the nonlinear flow features due to higher wave height or above-water hull configurations without any simplification. Since these nonlinear flow features considerably contribute to ships performance characteristics especially in the shorter wave range, it is important to take into account these features in a proper manner. Thus the availability of the CFD code has recognized quite important to achieve highly accurate sea-keeping performance predictions. In this paper, examples of validation study of a CFD simulation method are presented for merchant ships under sea-going conditions.

In Universal Shipbuilding Corporation, the CFD code named WISDAM-X (Orihara and Miyata (2003)) has been developed for the estimation of ship motions and hydrodynamic forces in waves. In the WISDAM-X code, Reynolds-Averaged Navier-Stokes (RANS) equation and the continuity equation are solved on the overlapping grid system using finite-volume descretization. Free-surface treatment is based on the density-function method (DFM) (Miyata et al. 1988). Using DFM, it is not necessary to fit the computational grid to the free surface and the arbitrary three-dimensional free-surface deformations can be treated without re-generation of the grid system.

In the following, a description of the WISDAM-X code is first presented. Then, results of validation study for WISDAM-X code are presented for the cases of a large-scale merchant ship. To obtain detailed validation data, model experiment is conducted for the measurement unsteady hull-surface pressures. Comparisons with experimental data are made of hull-surface pressures in regular head waves. Then, simulations are conducted of a tanker model in ballast conditions advancing in head waves. Examinations of computed flow structures are conducted to investigate the mechanism of increase in added resistance in ballast conditions. Experiment is also conducted for the measurement of ship motions and added resistance in ballast condition. Comparison of computed results with the measured data is performed for the evaluation of the accuracy of CFD simulations. Finally, conclusions obtained from this study are presented.

WISDAM-X METHOD

In the WISDAM-X method, an overlapping grid system is employed to implement rigorous wave generation, the

Corresponding author: *Hideo Orihara*
e-mail: *orihara-hideo@u-zosen.co.jp*

interactions of ships with incident waves and the resultant ship motions.

Since the details of the computational procedure of the WISDAM-X method are explained in Orihara and Miyata (2003), they are described here only briefly in the following.

In the WISDAM-X method, Reynolds-Averaged Navier-Stokes (RANS) equation and the continuity equation are solved on the overlapping grid system using finite-volume descretization. The RANS and the continuity equations formulated in non-inertial coordinate system. All of the fluid variables are made dimensionless with respect to the constant reference velocity $\boldsymbol{U}_0$, the ship length $\boldsymbol{L}$ and the density of fluid.

For the turbulent closure of the governing equations, eddy-viscosity type Baldwin-Lomax algebraic turbulence model (Baldwin and Lomax, 1978) is employed.

The free-surface treatment is based on the density-function method (DFM) developed by Miyata et al. (1988). DFM is a kind of front capturing methods and treats the time-historical evolution of the free surface by solving the following transport equation of the scalar variable ρ_m called density function;

$$\int_{\Omega} \frac{\partial \rho_m}{\partial t}\, dV = -\int_{\partial\Omega} \rho_m \boldsymbol{u}\cdot\boldsymbol{dS} \tag{1}$$

where $\boldsymbol{u}$ is the velocity vector of fluid. ρ_m is defined in the entire computational region as;

$$\rho_m = \begin{cases} 1, & \text{in the fluid region} \\ 0, & \text{otherwise} \end{cases} \tag{2}$$

Using DFM, it is not necessary to fit the computational grid to the free surface and the arbitrary three- dimensional free-surface deformation can be treated without re-generation of the grid system.

In order to implement the interaction of a ship with incident waves and the resultant ship motions, an overlapping grid system is employed in the WISDAM-X method. By employing the overlapping grid method, the overall computational domain is divided into two solution domains. The inner solution domain covers the region in the vicinity of the hull. The outer solution domain extends to the outer boundary, which is placed several ship's lengths away from the hull surface. In each solution domain, the computational grid is generated independently. The generation of the inner grid was made by the GMESH grid generation code developed at the National Maritime Research Institute (Kodama 1988, 1996).

The treatments of incident waves are conducted by specifying the fluid velocity components and wave height explicitly at the inflow boundary of the solution domain. The wave height and fluid velocity components are calculated by the linear wave theory. At the inflow boundary, the values of the density function are determined so that the vertical location of the iso-surface of ρ_m=0.5 coincides with the wave height.

The motion of the ship is simultaneously solved by combining the equations of motion of the ship body with the flow computation. Since the non-deforming grid is used, the flow computation in the near field is performed on the non-inertia coordinate system fixed to the body of the ship. The effect of the ship motion on the flow solution is taken into account by adding inertia forces as the body force term in the RANS equation.

In the WISDAM-X method, a PID (Proportional, Integral and Derivative) control is implemented for keeping time-averaged ship advancing speed $\overline{U}$ during surging motion in waves. This simulates the artificial thrust force needed to keep the determined time-averaged speed in waves. Based on the current and determined time-averaged advancing speeds of the ship, the following thrust command $T_{WV,C}(t)$ is given as:

$$T_{WV,C}(t) = k_P \Delta\overline{U} + k_P \frac{\partial\left(\Delta\overline{U}\right)}{\partial\, t} + k_I \int_0^t \Delta\overline{U}\, \boldsymbol{d}\tau + T_{WV,0} \tag{3}$$

where k_P is the gain coefficient for the proportional term; k_D is the gain coefficient for the derivative term; k_I is the gain coefficient for the integral term; $\Delta\overline{U}$ is the difference of averaged speed of the ship in waves $\left(= \frac{1}{\Delta T}\int_{t-\Delta T}^{t} \left(U(t) - U_0\right) d\tau\right)$; $U(t)$ is the current ship advancing speed; U_0 is the determined ship advancing speed. For the control of surging motion, the thrust command given by Equation (3) is added to the surging equation of motion.

PREDICTION OF BOW PRESSURES AND SHIP MOTIONS IN HEAD WAVES

In order to examine the accuracy for the prediction of unsteady flow-field around a moving ship in waves, bow surface pressure is predicted for a wide range of wave conditions. The computed results are thoroughly validated by comparing directly with the measured time histories of surface pressures obtained from the model experiment.

Condition of simulations

SR221C tanker model (e.g. Kashiwagi et al., 2004) is chosen for the calculations since it has a typical hull form of today's large oil tankers. The calculations are conducted on the overlapping grid system consisting of the inner and outer grids, as shown in Fig. 1. The numbers of grid points allocated for the grids is 133×30×89 and 141×41×101 for the inner and the outer grids, respectively.

The calculations are conducted in regular head waves at Fn=0.150 and Re=1.0×10^6. The length and amplitude of incident waves are set at ζ_A/L=0.01. The ship is set free to heave, pitch and surge. The flow is accelerated to a steady

advancing condition during the computational time T=0.0 to T=4.0, where T is made dimensionless with respect to (L/U_0). The wave computations start at T=5.0 and continued until T=20.0. Surge motions is restrained until T=5.0+8Te, where Te is the encounter period. Then the model is released free to surge.

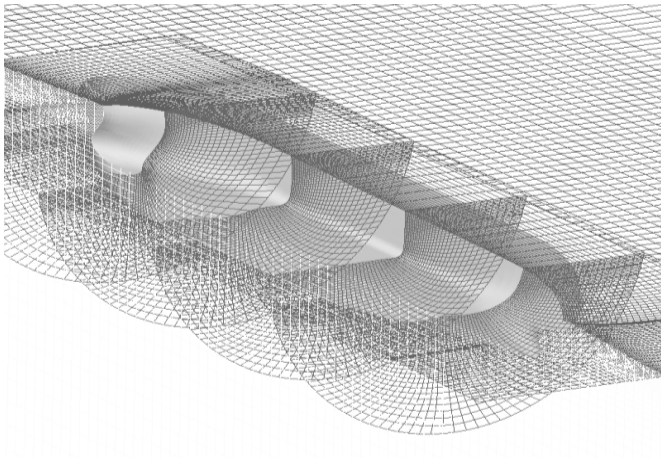

Fig. 1 Overlapping grid system for CFD simulations of a SR221C tanker model.

Description of the experiment

The experiment is conducted in a towing tank at Tsu Ship Model Basin (TSMB) of Universal Shipbuilding Co. The principal dimensions of the towing tank are $L\times B\times D$ = 240m×18m×8m. A flap-type wave-maker is located at the end of the tank and it generates regular waves propagating toward the model so that the condition of head seas is achieved. A 4.6m scale wooden model of SR221 tanker, shown in Fig. 2, is used for the experiment. In order to measure hull surface pressures in waves, nine pressure gauges (designated as P1 ～ P9, respectively) are installed on the model in the vicinity of the hull as shown in Fig. 3.

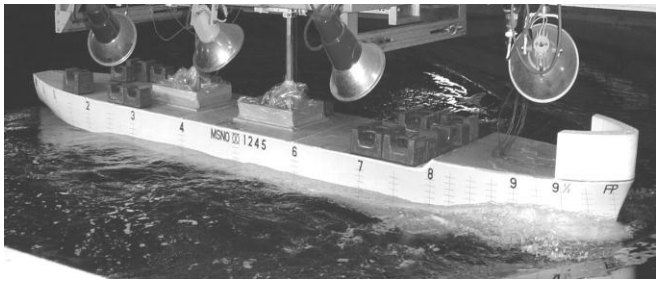

Fig. 2 SR221C tanker model towed in waves.

Three gauges ($P1$～$P3$) are placed at the fore end of the ship. The other six gauges are placed at three hull square stations (S.S.) 9 3/4, 9 1/2 and 9. All the pressure gauges are placed above the still water surface. The model is attached to the towing carriage and towed on the bare hull condition without a propeller and a rudder. The model is allowed to heave, pitch and surge, but roll, sway and yaw are restricted. In the experiment, the measurements are conducted in regular head waves with wave length to ship length ratio (λ/L) of 0.4 to 2.0 and wave amplitude to ship length ratio (ζ_A/L) of 0.01. For all the cases, the model is towed at a constant speed of Froude number, Fn = 0.150.

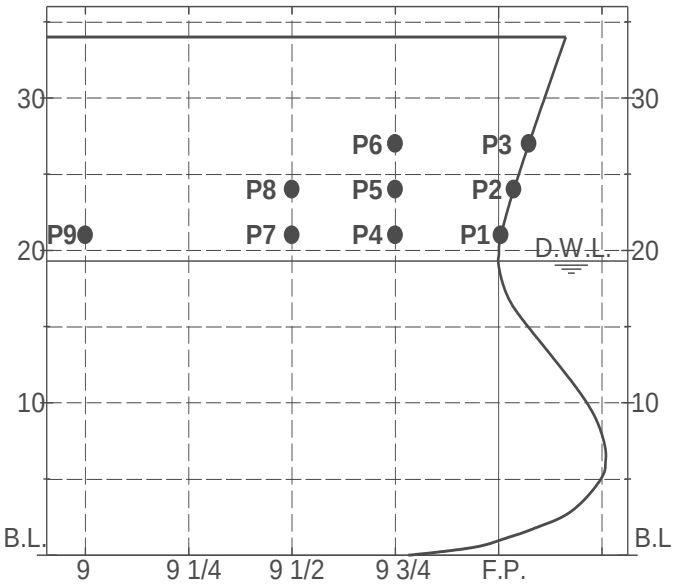

Fig. 3 Locations of pressure measurement on SR221C.

Results and discussion

Comparisons of time histories of hull surface pressures are shown in Figs 4 and 5 for the cases of λ/L=0.6, 1.0, respectively. In the present study, the pressures are defined as the difference relative to the atmospheric pressures. So the pressures are zero when the pressure gauges exposed in the air. Since the gauges are placed above the still water level (see Fig. 3), all the gauges experienced the exposure in the air for both cases of wave lengths. As can be seen in the figures, computed results (shown in bold lines) are in good agreement with the experimental data (shown in dotted lines). The calculated histories capture quite well the change in the shape of pressure time histories from triangular shape to rounded one with the increase of the length of incident waves.

Comparisons of the surface pressure amplitudes are shown in Fig. 6, where pressure amplitudes are defined as the difference between the maximum and minimum values of time histories and normalized by the amplitude of the incident wave. The experimental data is obtained by averaging over several encounter periods of the incident wave. The agreement of the calculated results with the experimental data is quite well for all the pressure measurement points except for the case of λ/L=0.4. It is noted that at the fore end of the hull ($P1$～$P3$), the computed pressure coincides well with the experimental data. Since the accurate prediction of surface pressure near the bow is quite important for the added resistance and local wave loads of the ship for structural analysis, the present result may demonstrate the advantage of the present CFD method.

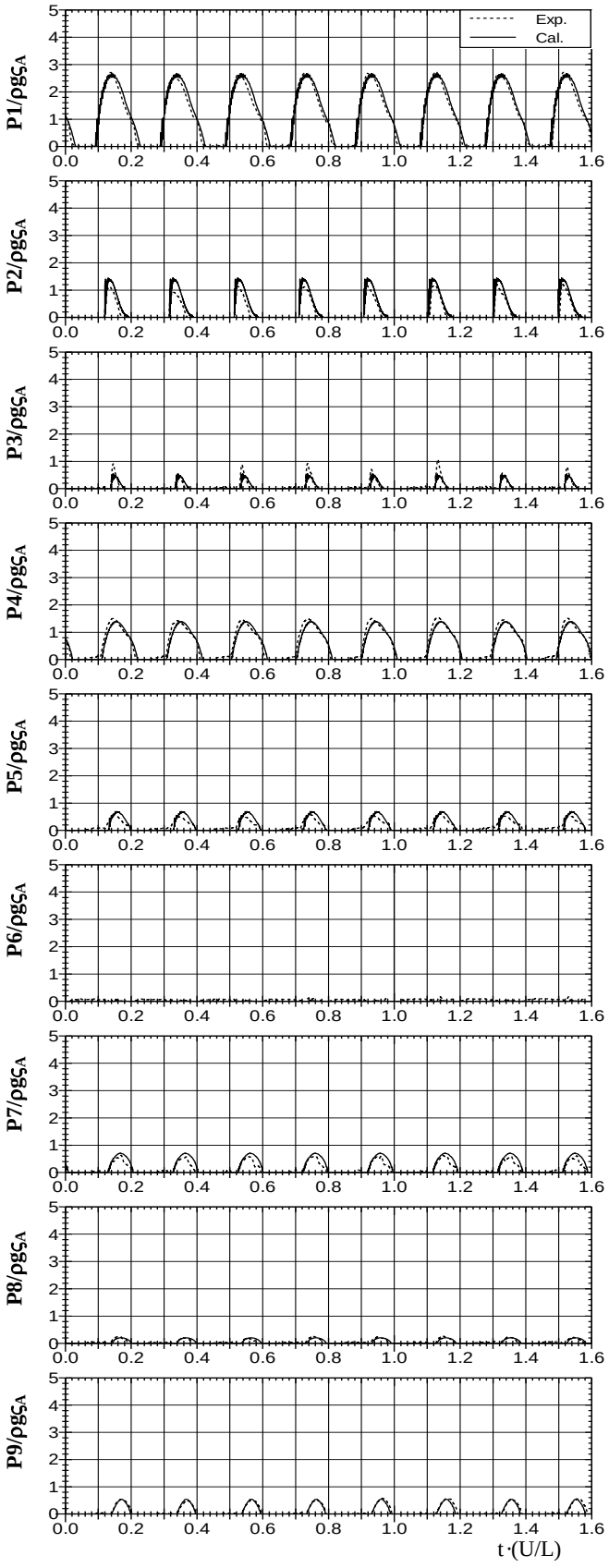

Fig. 4 Comparison of time-historical variation of surface pressures on a SR221C tanker in regular head waves of λ/L=0.6 and ζ_A/L=0.01.

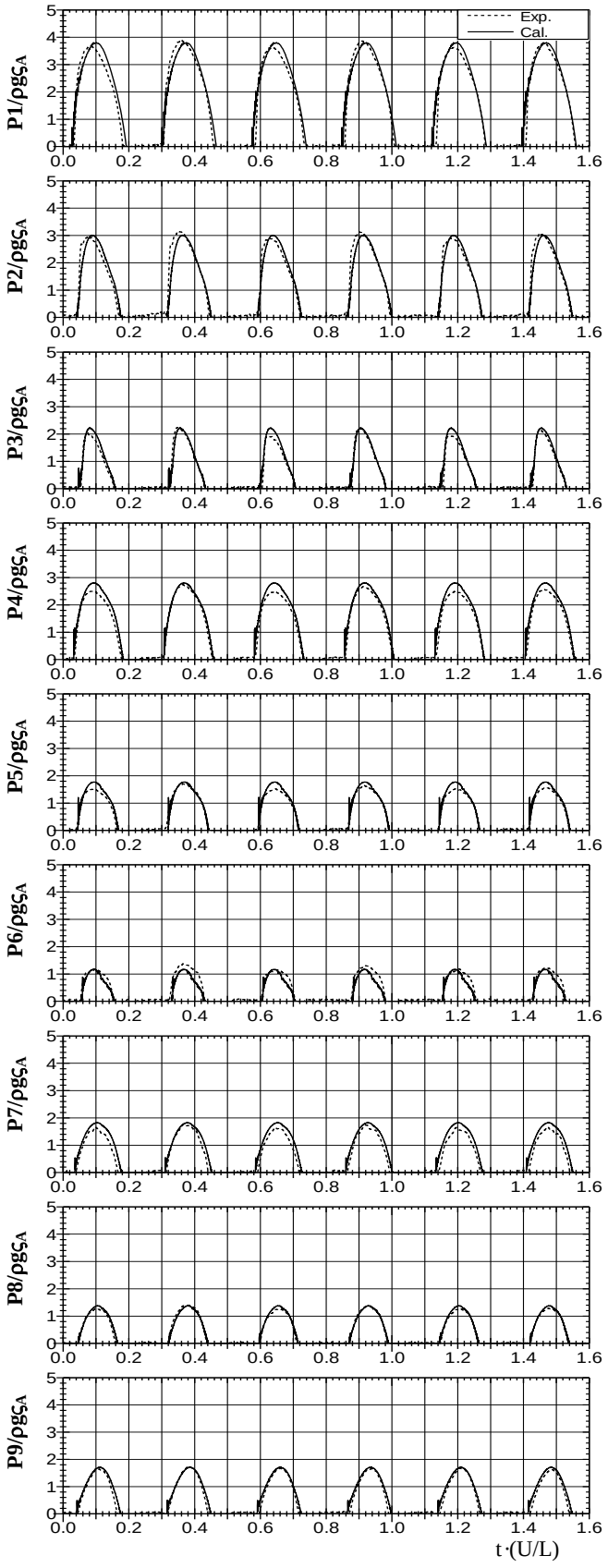

Fig. 5 Comparison of time-historical variation of surface pressures on a SR221C tanker in regular head waves of λ/L=1.0 and ζ_A/L=0.01.

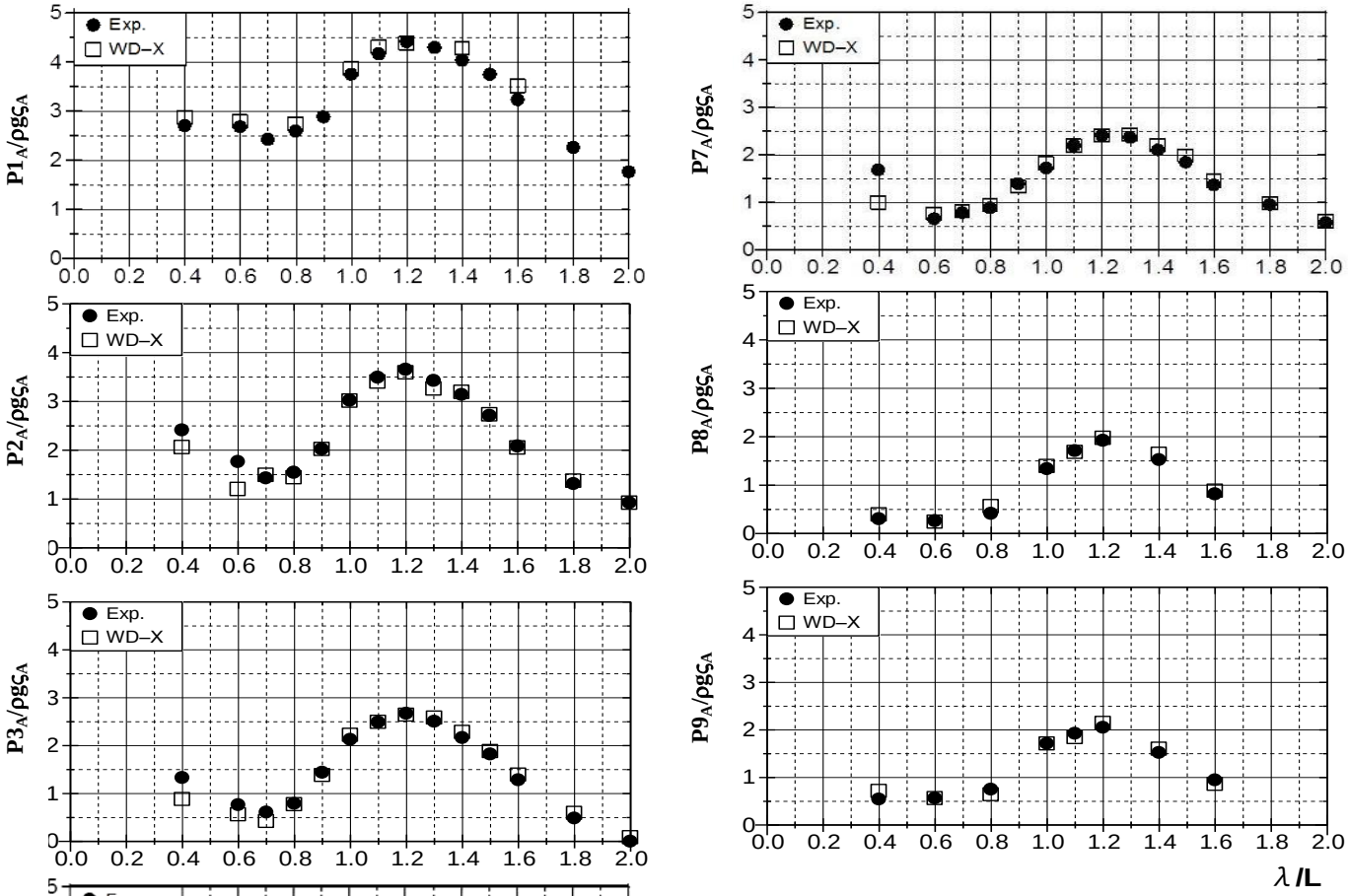

Fig. 6 Comparison of time-historical variation of surface pressures on a SR221C tanker in regular head waves of λ/L=1.0 and ζ_A/L=0.01.

PREDICTION OF SHIP MOTIONS AND ADDED RESISTANCE IN BALLAST CONDITION

Condition of simulations

SR221C tanker model is chosen for the calculations. All the calculations are conducted on the overlapping grid system consisting of the inner and outer grids. The numbers of grid points allocated for the grids is $133\times30\times89$ and $141\times41\times101$ for the inner and the outer grids, respectively.

The calculations are conducted in regular head waves at Fn=0.150 and Re=1.0×10^6. The length and amplitude of incident waves are $0.4 \leqq \lambda/L \leqq 2.0$ and ζ_A/L=0.01, respectively. The ship is set to be free in heave, pitch and surge modes. The time increment is set at a normalized value of 0.0002 based on reference time $T(=L/U_0)$. The flow is accelerated to a steady advancing condition during the computational time T=0.0 to T=4.0. The wave computations start at T=8.0 and continued until T=16.0. Surge motions is restrained until T=8.0+8Te, where Te is the encounter period. Then the model is released free to surge.

Description of the experiment

The experiments are carried out in the towing tank at TSMB. A wooden model of SR221C tanker (the same model used for the pressure measurement is used in the experiment. The model is attached to the towing carriage so that it can move freely in heaving, pitching and surging modes. The model is dynamically balanced so that the weight and longitudinal radius of gyration in pitch direction coincide with those of the normal ballast condition.

The experiments are carried out in regular head waves over a range of its length and height. The incident-wave amplitudes are set at 0.01L throughout the experiment. The wave length to ship length ratio (λ/L) is varied from 0.4 to 2.0. Throughout the experiments, the model is towed at a constant speed of 1.02 *m/s*. The corresponding Froude number based on the model length is 0.15.

Results and discussion

Time evolutions of computed surface pressure distributions in head waves of λ/L=0.6 and 1.0. are shown in Fig. 7. In the figures, pressure distributions are shown at an interval of 1/4 of the encounter period (*Te*).

As shown, time-sequential variations of the surface pressure distributions are remarkable in the longer wave case λ/L=1.0, where the upper surface of the bow bulb is fully submerged under the water surface and higher pressure regions are observed. It is also noted that large portion of bow bottom is emerged from the water surface. On the other hand, in the short wave of λ/L=0.6, variations in surface pressures and water surface heights are relatively small.

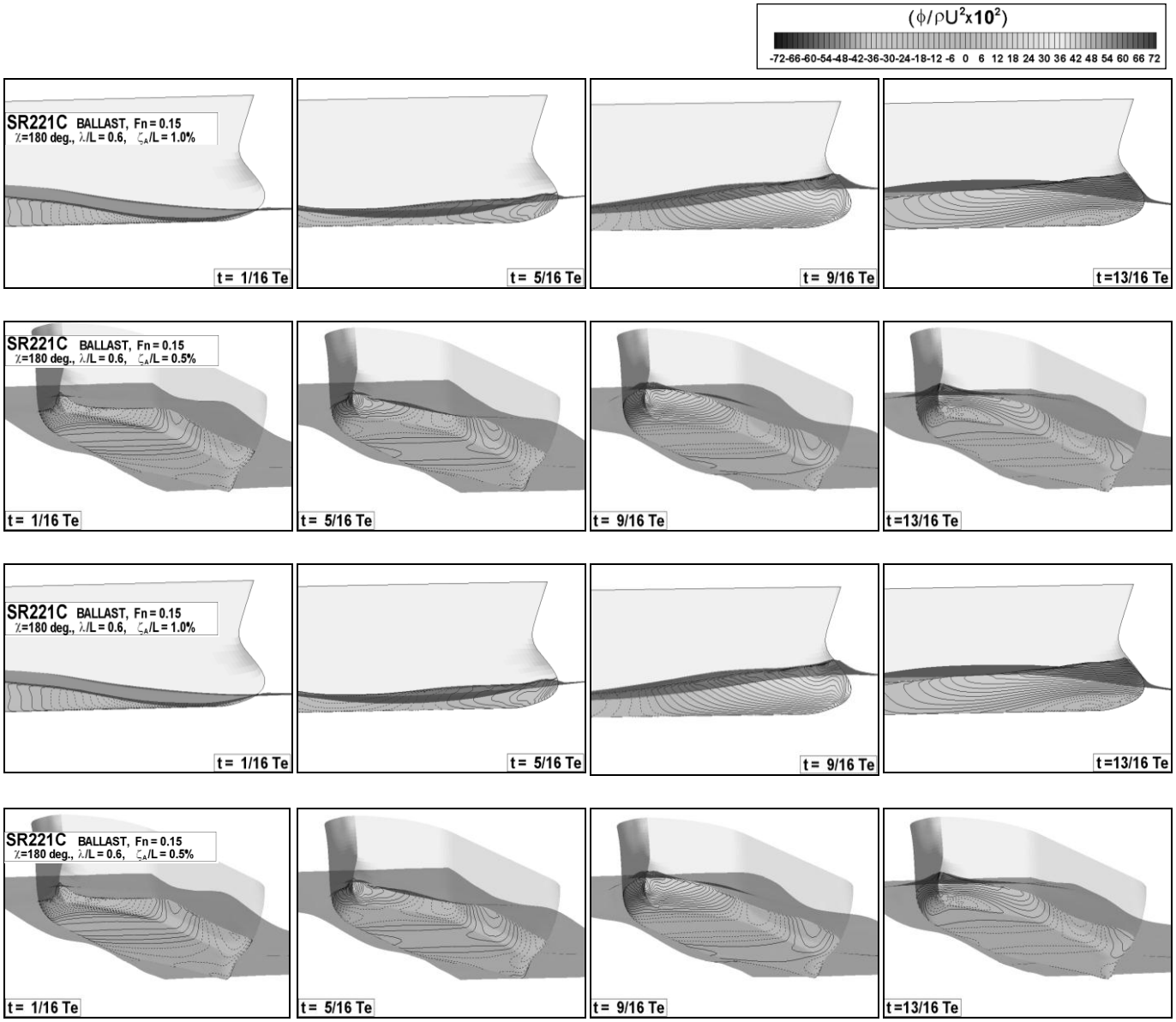

Fig. 7 Comparison of time-evolutions of computed pressure contour maps on a SR221C model in regular head waves of ζ_A/L=0.01 and λ/L=0.6, 1.0, *Fn*=0.15.

Comparisons of computed ship's heaving (ξ_3) and pitching (ξ_5) motions with the experiment are shown in Fig. 8, where heaving and pitching motion amplitudes are made dimensionless with respect to incident wave amplitudes (ζ_A) and wave slope amplitude ($k\zeta_A$), respectively.

Phase differences are defined with respect to that of incident waves at the ship's center of gravity. As clearly seen in the figures, ship motions are accurately predicted by CFD simulations in terms of amplitudes and phases. It is noted that the heave motion amplitudes increases monotonously with λ/L and there is no clear peak of heave amplitude which typically occurs in heaving motion around λ/L=1.0 in fully-loaded conditions.

Comparison of the added resistance are shown in Fig. 9, where calculated and measured added resistances are normalized with $\rho g\zeta_A^2(B^2/L)$ and shown as a function of λ/L. While the calculated results slightly overestimate the experiment in wave range less than λ/L<1.0, calculated results reproduce reasonably well the experimental data including the short wave range where the diffraction component is dominant in the added resistance. As pointed out by Kashiwagi et al. (2004), it has been well known that there exist noticeable discrepancies in the prediction by conventional methods of the added resistance in short waves of a full-form ship like SR221C in ballast condition. The reasonable agreement in the short wave range may be due to the exact treatment of the nonlinear hull surface and the free-surface conditions employed in the CFD simulation.

Since tankers and bulk carriers are usually operated in ballast conditions as simulated in this section for approximately half of its commercial life due to their operational pattern, the accurate performance prediction in ballast condition has a significant importance for the development superior performance in a seaway. The availability of WISDAM-X for the prediction of added resistance in ballast condition demonstrated herein may contribute to the achievement of this goal.

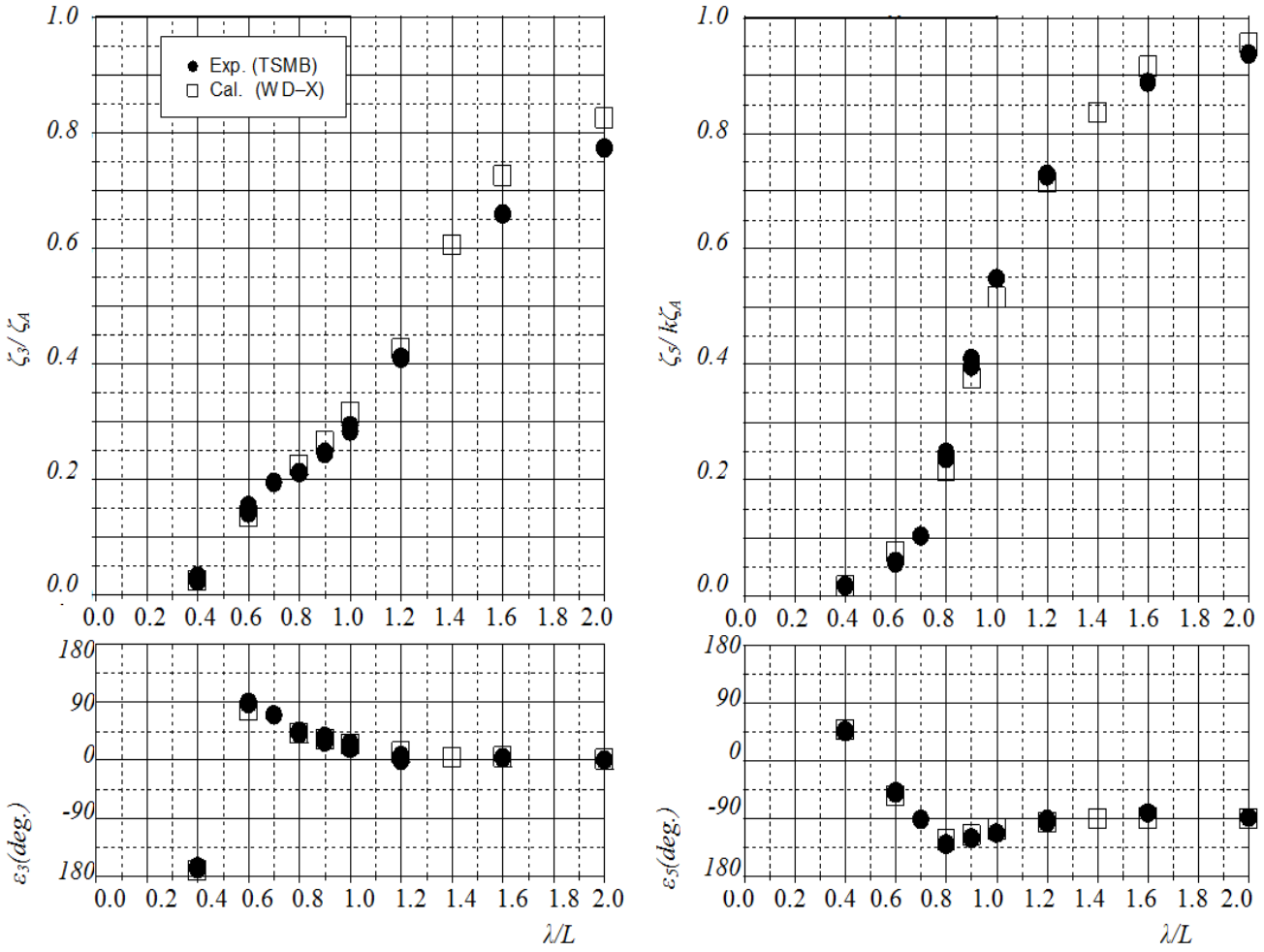

(a) Pitch; χ=180˚ (b) heave; χ=180˚

Fig. 8 Comparison of RAOs of heave and pitch for a SR221C model in ballast condition, *Fn*=0.15, $\zeta A/L$=0.01.

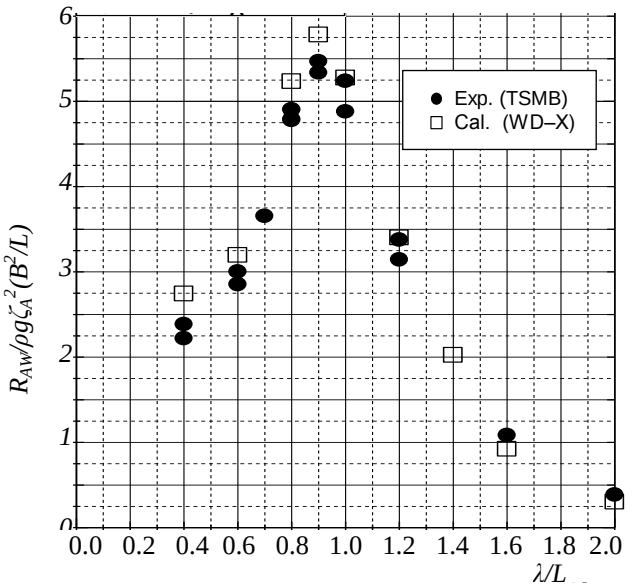

Fig. 9 Comparison of RAOs of added resistance for a SR221C model in ballast condition, Fn=0.15, ζ_A/L=0.01.

CONCLUSIONS

Unsteady CFD simulations have been conducted of flows and motions of a merchant ship model advancing in waves using a RANS code called WISDAM-X to examine the availability of WISDAM-X as a tool for the prediction of sea-keeping performance and its applicability to the development of hull-forms with superior performance under realistic operating conditions.

Examples of validation study of WISDAM-X code are presented for two cases of CFD simulations for a large tanker model, and the simulation results are compared with the experimental data.

First, computed hull-surface pressures are compared with the experimentally measured data. Surface pressure time-histories on the above waterline portion are examined over a range of wave length under head wave conditions. As a measure for the magnitude of the pressures acting above the waterline, pressure amplitude operator is defined and evaluated form both simulated and measured time-histories. Simulated results correlate fairly well with the experimental data in terms of time-histories and amplitude operators.

Then, simulations for a tanker model in ballast conditions are conducted and examinations of computed flow structures are conducted to investigate the mechanism of increase in added resistance in ballast conditions.

Accuracy of the computations is evaluated by comparing with the experimental data. It is shown that the degree of agreement with the experiment is satisfactory for ship motions and added resistance. Good accuracy in the prediction of ship motions and added resistance obtained from the present examination seems to indicate the availability of WISDAM-X code as a tool for the prediction of sea-keeping performance and its application to the development of ships with superior ocean-going qualities.

ACKNOWLEDGEMENTS

The author would like to thank members of Testing & Analyzing Section of Technical Research Center of Universal Shipbuilding Co. for their help in conducting model experiments at TSMB.

REFERENCES

Baldwin, B. and Lomax, T., 1978. Thin-layer approximation and algebraic model for separated turbulent flows. *AIAA-Paper* 78-0257.

Kashiwagi, M. Sugimoto, K. Ueda, T. Yamasaki, K. Yamashita, R. Ito, A. and Mizokami, S., 2004. An analysis system for propulsive performance in waves. *Journal. of the Kansai Society of Naval Architects, Japan*, No.241, pp. 67-82.

Kodama, Y., 1988. Three-dimensional grid generation around a ship hull using the geometrical method. *Journal of the Society of Naval Architects of Japan*, 164, pp. 1-8.

Kodama, Y., 1996. Representation of ship hull form using a multi-block grid. *Journal of the Kansai Society of Naval Architects*, No. 226, pp. 85-90.

Miyata, H. Katsumata, M. Lee, Y.G. and Kajitani, H., 1988. A finite-difference simulation method for strongly interacting two-phase flow. *Journal of the Society of Naval Architects of Japan*, 163, pp. 1-16.

Orihara, H. and Miyata, H., 2003. Evaluation of added resistance in regular incident waves by computational fluid dynamics motion simulation using an overlapping grid system. *Journal of Marine Science and Technology*, 8, pp. 47-60.